AMCoR

Universal optimal hole-doping concentration in single-layer high-temperature cuprate superconductors

Honma, T; Hor, PH

Universal optimal hole-doping concentration in single-layer high-temperature cuprate superconductors

T Honma[1][2] **and P H Hor**[1]

[1] Texas Center for Superconductivity and Department of Physics,
University of Houston - Houston, TX. 77204-5002, USA
[2] Department of Physics,
Asahikawa Medical College - Asahikawa, Hokkaido 078-8510, Japan

E-mail: `homma@asahikawa-med.ac.jp`, `phor@uh.edu`

Abstract. We argue that in cuprate physics there are two types, hole content per CuO_2 plane (P_{pl}) and the corresponding hole content per unit volume (P_{3D}), of hole-doping concentrations for addressing physical properties that are two-dimensional (2D) and three-dimensional (3D) in nature, respectively. We find that superconducting transition temperature (T_c) varies systematically with P_{3D} as a superconducting "*dome*" with a universal optimal hole-doping concentration $P_{3D}^{opt.} = 1.6 \times 10^{21}$ cm^{-3} for single-layer high temperature superconductors. We suggest that $P_{3D}^{opt.}$ determines the upper bound of the electronic energy of underdoped single-layer high-T_c cuprates.

1. Introduction

In high-temperature cuprate superconductors (HTS) the hole-doping concentration is the single most important physical parameter that dictates the cuprate physics. It has been a subject of extensive studies since the beginning of the HTS era until today. It is also evident from the existence of the robust generic electronic properties *vs.* hole-doping concentration phase diagram [1]. In spite of its fundamental important role in studying HTS, there is no consistent and simple method to determine hole-doping concentration for all HTS.

HTS consist of one, two and more conductive "*CuO₂ plane*" layers sandwiched between blocks of insulating "*charge reservoir*" layers generally referred as single-, double- and multi-layer HTS, respectively. Cation-doping and/or oxygen-doping within the charge reservoir introduce holes into the CuO₂ plane. In general, the doped-holes are expressed as the *hole content per CuO₂ plane* (P_{pl}). Note that P_{pl} so defined is intrinsically a two-dimensional (2D) quantity. In the cation doped HTS, the P_{pl} can be directly determined from the doped cation content, such as $P_{pl} = x$ in the Sr-doped La$_{2-x}$Sr$_x$CuO$_4$ (SrD-La214). However, in the oxygen-doped (OD-) or cation/oxygen co-doped (CD-) HTS, it is highly non-trivial to determine P_{pl}. Because, for La$_{2-x}$Sr$_x$CuO$_{4+\delta}$, P_{pl} depends on the excess oxygen content (δ), but the doping efficiency of oxygen atoms depends on the type of charge reservoir and/or P_{pl} [2, 3].

Superconducting transition temperature (T_c) *vs.* P_{pl} for the SrD-La214 shows a dome-shaped curve with a maximum T_c (T_c^{max}) of ~ 37 K at $P_{pl} \sim 0.16$. Many other HTS also exhibited the similar dome-shaped curve, although the T_c^{max} depends on the HTS materials. It was then conjectured that all HTS follow a universal dome-shaped curve with T_c^{max} at $P_{pl} = 0.16$ [4]. Subsequently, the hole concentration (P_{T_c}), considered to be identical to P_{pl}, was conveniently estimated by $T_c(P_{T_c})$-scale using eq. (1).

$$\frac{T_c}{T_c^{max}} = 1 - 82.6\big(P_{T_c} - 0.16\big)^2. \tag{1}$$

Most recently, based on the thermoelectric power at room temperature (S^{290}), a universal $S^{290}(P_{pl})$-scale (hereafter P_{pl}-scale) is constructed as new scale that is different from the $T_c(P_{T_c})$-scale (hereafter P_{T_c}-scale) [5]. The distinct features of P_{pl}-scale are: (a.) pseudogap temperatures become universal to all HTS and depend only on P_{pl}, and (b.) T_c^{max} is no longer universally pinned at $P_{pl} = 0.16$, it depends on the specific material system of HTS [5]. Therefore P_{pl} can be regarded as a carrier scale dictated by the pseudogap energy scale. In contrast the P_{T_c}-scale is based on the energy scale of T_c^{max}. Since pseudogap phase is the precursor of high-T_c superconductivity, it seems to be plausible that P_{pl} is the proper carrier scale for both normal and superconducting properties of layered cuprates. If so, then we expect the P_{pl}-scale should recover the experimentally observed dome-shaped $T_c(P_{T_c})$ curve. In this letter, we show that P_{pl}, with a straight forward extension of P_{pl} to an effective three-dimensional (3D) hole concentration, can indeed describe the universal dome-shaped $T_c(P_{T_c})$ curve.

We define a 3D hole concentration (P_{3D}) in terms of P_{pl} in eq. (2).

$$P_{3D} \equiv P_{pl} \times \left(\frac{N_l}{V_{u.c.}}\right). \tag{2}$$

Here, $V_{u.c.}$ and N_l are the unit cell volume and the number of CuO_2 plane per unit cell, respectively. Since P_{3D} is defined on the universal 2D P_{pl}-scale, this definition has qualitatively taken into account the charge de-confinement effect of the holes in cuprates. Therefore P_{3D} can be viewed as the "*effective*" 3D hole-doping concentration even when holes are completely confined in CuO_2 *planes*.

In this letter we make a clear distinction between P_{pl}, hole content per CuO_2 plane, and the corresponding effective 3D hole-doping concentration (P_{3D}) defined in eq. (2). We show that it is important to use the physically relevant hole-doping concentration in order to visualize the intrinsic and systematic doping behaviors of any physical property of HTS. Furthermore, we show that the $\frac{T_c}{T_c^{max}}$ *vs.* P_{3D} exhibits a universal dome-shaped curve with the universal optimal hole-doping concentration $P_{3D}^{opt.} = 1.6 \times 10^{21}$ cm^{-3} for single-layer HTS. We find that the P_{T_c}-scale is identical to the P_{3D}-scale and should be understood in the context of a normalized effective 3D carrier concentration. In this report we will focus only on the single-layer HTS. The extension of our definition of P_{3D} for the multi-layer HTS with equivalent CuO_2 planes is straight forward.

2. Experimental

P_{pl} of data collected from the literatures [6, 7, 8, 9, 10, 11, 12, 13, 14, 15, 16, 17, 18, 19] are reliably determined by P_{pl}-scale. Some of the data plotted in Fig. 1 and 3 are coming from the literatures [20, 21, 22, 23] where only T_c is reported. Their P_{pl} are estimated from the $T_c(P_{pl})$ curve plotted in Fig. 2(a). For the calculation of P_{3D}, we use the typical value of 190 Å^3, 345 Å^3, 355 Å^3 and 143 Å^3 for the unit cell volume of SrD-La214 with N_l = 2 [7], $Tl_2Ba_2CuO_{6+\delta}$ (OD-Tl2201) with N_l = 2 [24], $Bi_2Sr_{2-x}La_xCuO_{6+\delta}$ (CD-Bi2201) with N_l = 2 [25], and $HgBa_2CuO_{4+\delta}$ (OD-Hg1201) with N_l = 1 [26], respectively.

3. Results and discussion

We start with a comparison of our scale to in-plane Hall number ($n_H = \frac{1}{|e|R_H}$), where R_H is in-plane Hall coefficient and $|e|$ is electron charge, that estimates carrier number per unit *volume*. In the single-layer SrD-La214 and OD-Tl2201, the R_H of the polycrystalline samples is experimentally confirmed to be corresponding to the in-plane R_H of the single crystals [16, 27]. In Fig. 1(a), we plot the n_H as a function of P_{3D} for the single-layer HTS. For SrD-La214 [13, 14, 15, 16], there are three linear $n_H(P_{3D})$ regimes (regime-I, II and III). In regime-I for $P_{3D} \leq 5.5 \times 10^{20}$ cm^{-3}, n_H is identical to P_{3D}. This is very encouraging and indicates that the P_{3D} defined here is physically sound and quantitatively valid. At $P_{3D} = 5.5 \times 10^{20}$ cm^{-3}, the slope of linear $n_H(P_{3D})$ suddenly changes from 1 to ~3.2. In the regime-III for $P_{3D} \geq 1.6 \times 10^{21}$ cm^{-3}, the linear $n_H(P_{3D})$ changes slope to 25. The observed rapid increase in R_H may related to
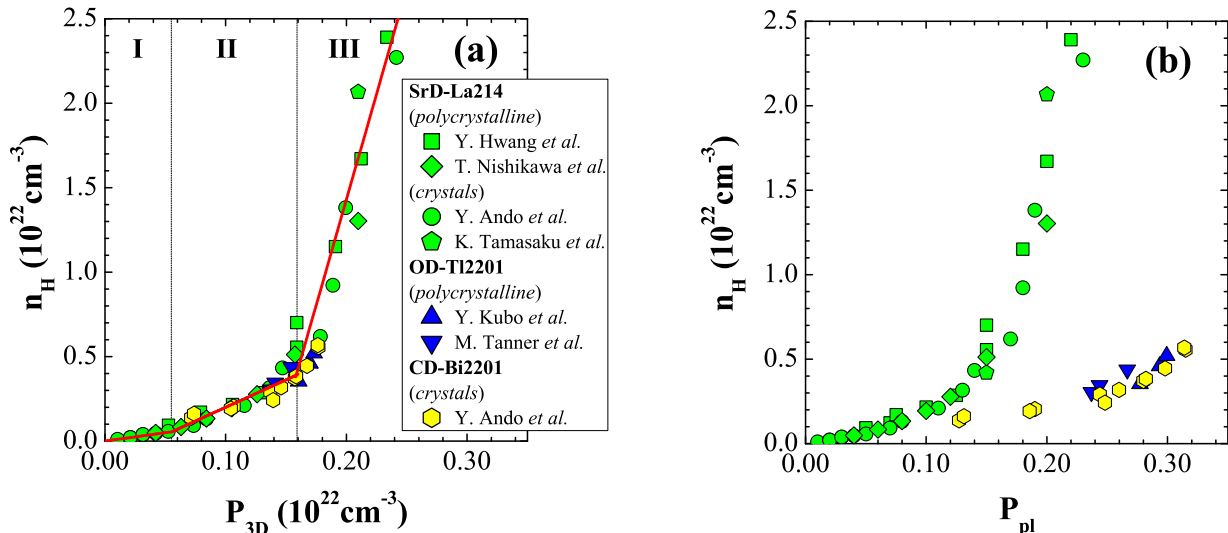
Figure 1. (Colour online) (a) Hall number (n_H) as a function of P_{3D} for the single-layer HTS. The slope of solid lines is 1 in regime-I, 3.2 in regime-II and 25 in regime-III. The data for SrD-La214 are extracted from ref. [13, 14, 15, 16]; CD-Bi2201 from ref. [8, 11, 12]; OD-Tl2201 from ref. [17, 23]. The P_{pl} of OD-Tl2201 by Kubo *et al.* [23] is estimated from the $T_c(P_{pl})$ curve. The dotted lines show $P_{3D} = 5.5\times10^{20}$ cm^{-3} and 1.6×10^{21} cm^{-3}. (b) Same data as in graph (a) are plotted as a function of P_{pl}.

the change in sign of R_H observed in the overdoped SrD-La214 [16]. The three regimes clearly define three distinct electronic states of doped holes. The identical trend is also observed in CD-Bi2201 crystals [8, 11, 12] and OD-Tl2201 ceramics [6, 17, 23]. We need to emphasize that this systematic behavior is not governed by the P_{pl}, but by the P_{3D}. In Fig. 1(b) we plot the same data set of n_H as a function of P_{pl}. The n_H for CD-Bi2201 and OD-Tl2201 do not follow that of SrD-La214, and the three physically distinct regimes can not be resolved.

Since it is well known that the electronic anisotropy decreases with doping in all HTS, the above observations suggest that there are three distinct confinement regimes of doped holes. In regime-I where n_H is the same as P_{3D} indicates doped holes are completely confined within the CuO$_2$ plane. For regimes-II and -III where $n_H = \alpha P_{3D}$ with a non-unity slope, $\alpha \sim 3.2$ and 25, respectively, each represents a distinct de-confinement regime of doped-hole states. Noted that the change of slope between two regimes is quite abrupt, more like a phase transition than some kind of crossover behaviors. The critical P_{3D} that define the boundary between regime-I and -II and the boundary between regime-II and -III actually correspond to the crtitical P_{3D} for the insulator-superconductor transition (P_{3D}^c) and $P_{3D}^{opt.}$, respectively. The physical meaning of each regime will become clear in our discussion of Fig. 2(b).

In Fig. 2(a), we plot T_c as a function of P_{pl}. Here, we use T_c value reported in the literature [6, 7, 8, 9, 10], irrespective of how it was defined. The optimal doping level
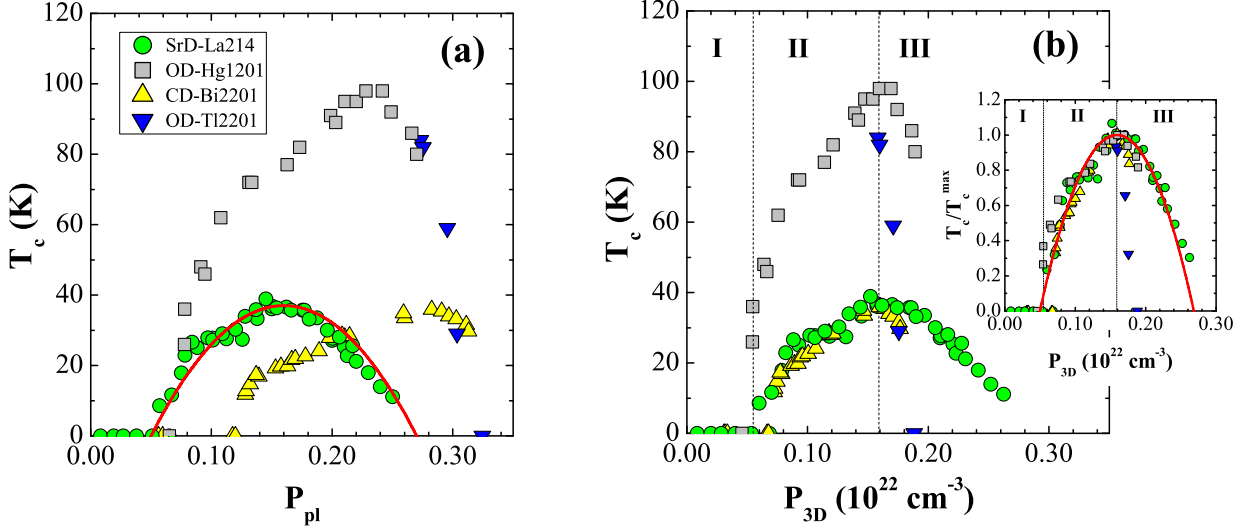
Figure 2. (Colour online) (a) Superconducting transition temperature (T_c) as a function of P_{pl} for the single-layer HTS. The data for SrD-La214 are extracted from ref. [7, 10]. The data set for OD-Hg1201, CD-Bi2201 and OD-Tl2201 are extracted from ref. [9], [8], and [6], respectively. The solid line shows T_c curve ($T_c^{max} = 37$ K) reproduced by using eq. (1). (b) Same data as in graph (a) are plotted as a function of P_{3D}. The dotted lines show $P_{3D} = 5.5 \times 10^{20}$ cm^{-3} and 1.6×10^{21} cm^{-3}. The inset shows the $\frac{T_c}{T_c^{max}}$ *vs.* P_{3D}. The solid line shows $\frac{T_c}{T_c^{max}}$ curve reproduced by using eq. (3).

strongly depends on the systems. Noted that the optimal doping levels for OD-Hg1201 and CD-Bi2201 are at $P_{pl} \sim 0.23$ and 0.28, respectively, although that for SrD-La214 is ~ 0.16. Thus, the optimal doping level for the single-layer HTS is not universally equal to 0.16, as reported in some earlier studies [5, 28]. However, the P_{T_c}-scale has been used successfully to discuss various characteristic properties of HTS [29]. We show that the P_{T_c} is actually related to P_{3D}.

To see that P_{3D} has real physical consequence we replot, in Fig. 2(b), T_c as a function of P_{3D} using the same data set of Fig. 2(a). The superconductivity appears at $\sim 5.5 \times 10^{20}$ cm^{-3}. The T_c^{max} universally appears at $\sim 1.6 \times 10^{21}$ cm^{-3}. The inset shows the $\frac{T_c}{T_c^{max}}$ *vs.* P_{3D}. The $\frac{T_c}{T_c^{max}}$ for SrD-La214, OD-Hg1201 and CD-Bi2201 follow the same dome-shaped curve. Now we can pin down the absolute value of 3D optimal hole-doping concentration in eq. (3) :

$$\frac{T_c}{T_c^{max}} = 1 - 83.64\left(P_{3D} \times 10^{-22} - 0.159\right)^2, \tag{3}$$

where the unit of P_{3D} is " cm^{-3} ". It is clear that the P_{T_c} determined in eq. (1) is not planar hole-doping concentration but physically identical to our defined P_{3D}. Therefore, we can understand why P_{T_c}-scale worked in the earlier doping-dependence studies. However, we need to emphasize that P_{T_c}-scale is the proper carrier scale for 3D "bulk" cuprate properties. The T_c of underedoped OD-Hg1201 may seem slightly to be
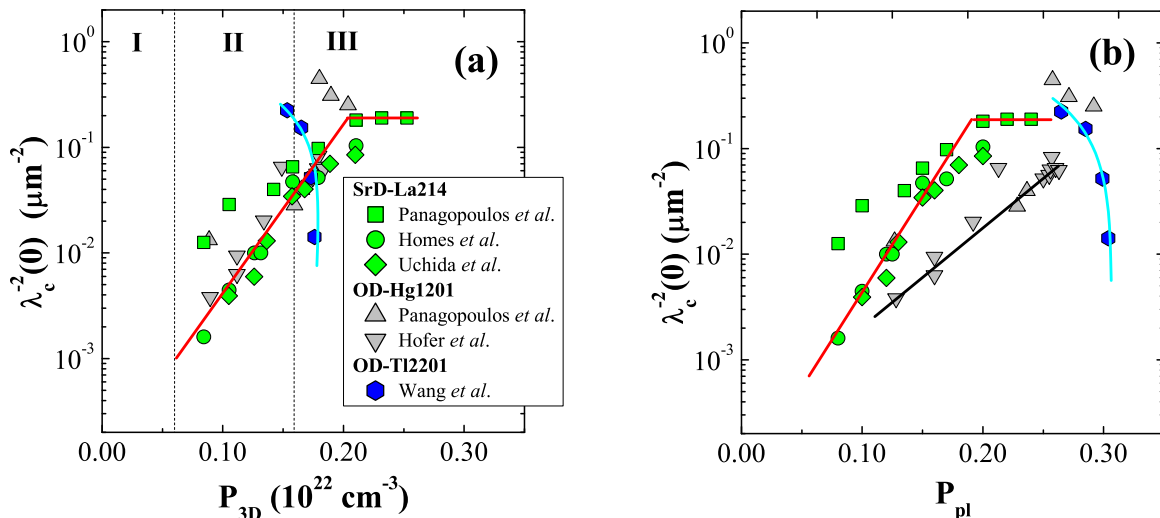
Figure 3. (Colour online) (a) *c*-axis logarismic inverse squared penetration depth ($\lambda_c^{-2}(0)$) as a function of P_{3D}. The data for SrD-La214 are extracted from ref. [18, 19, 21], OD-Hg1201 from ref. [21, 22] and OD-Tl2201 from ref. [20]. The dotted lines show $P_{3D} = 5.5 \times 10^{20}$ cm^{-3} and 1.6×10^{21} cm^{-3}. (b) Same data as in graph (a) are plotted as a function of P_{pl}. The solid lines are guide for the eyes.

higher than T_c calculated from eq. (3). OD-Hg1201 is the pure oxygen-doped compound, although CD-Bi2201 is the cation/oxygen co-doped compound. Accordingly, the oxygen atom within the charge reservoir is more mobile or softer in OD-Hg1201 [30, 31]. The slightly higher T_c could be due to the change in P_{pl} by the thermal oxygen re-arrangement [31].

To further demonstrate our point that we should use the hole-doping concentration of the correct dimensionality consistent with the very nature of the physical properties under study, we consider the inverse square of the *c*-axis penetration depth ($\lambda_c^{-2}(0)$). The *c*-axis superfluid density ($\lambda_c^{-2}(0)$), independent of the *c*-axis coupling mechanism, is intrinsically a 3D property of the HTS. In Fig. 3(a), we plot $\lambda_c^{-2}(0)$ on the logarithmic scale as a function of P_{3D} [18, 19, 20, 21, 22]. The $\lambda_c^{-2}(0)$ increases with doping until 2×10^{21} cm^{-3}, higher than $P_{3D}^{opt.}$, and either decreases or remains at a constant level beyond. In Fig. 3(b), we plot the same data set of $\lambda_c^{-2}(0)$ as a function of P_{pl}. In the underdoped side, the trend in $\lambda_c^{-2}(0)$ for OD-Hg1201 is different from that for SrD-La214. No systematic $\lambda_c^{-2}(0)$ *vs.* P_{pl} behaviors can be observed. Thus, the $\lambda_c^{-2}(0)$ is not governed by the P_{pl} but by the P_{3D}. Accordingly, the $\lambda_c^{-2}(0)$, independent of the *c*-axis coupling mechanism, is intrinsically a 3D property of the HTS. There are many studies based on the P_{T_c}-scale [29] and, to put them into proper prospective, these results should be understood in the context of P_{3D}.

The existence of a universal $P_{3D}^{opt.}$ has an interesting implication to the stability of underdoped electronic states, namely, it is the upper bound of the electronic energy

of single-layer HTS. Therefore there is a common physical origin, dictated by P_{3D}^{opt}, for the transition from underdoped to overdoped regimes. Note that $P_{3D}^{opt.}$ is an effective "3D" hole concentration that is intrinsically consistent with the dominance of Fermi liquid state in 3D electronic systems and the experimental observations that Fermi liquid behavior emerges beyond optimal doping concentration [32]. Using the simple free electron model with hole concentration equal to $P_{3D}^{opt.}$ [33], the corresponding Fermi energy is ~ 0.5 eV, close to the binding energy of the lower Hubbard band (~ 0.4 to 0.6 eV) of layered cuprates [34]. More specifically, as suggested in ref. [35], the ~ 0.5 eV is the energy required to promoting a hole from $d_{x^2-y^2}$ to $d_{3Z^2-r^2}$ to form $d - d^*$ exciton, another plausible channel for hole de-confinement.

4. Summary

We have shown that for HTS there are two types of hole-doping concentration depending on the dimensionality, that is, the effective 3D hole-doping concentration P_{3D} and hole content per Cu-O$_2$ plane P_{pl} defined in ref.[5]. Combining these two we have a complete working scale to address various physical properties for all HTS. Any 2D/in-plane property should be plotted as a function of P_{pl} and any 3D/out-of-plane property as a function of P_{3D}. Indeed, we see that $\lambda_c^{-2}(0)$ and the magnitude of T_c are governed by P_{3D}, while pseudogap physics is described by P_{pl} [5]. While the T_c^{max} is different for different single-layer HTS, we observed a universal $P_{3D}^{opt.} = 1.6 \times 10^{21}$ cm^{-3} for single-layer HTS that determines the stability limit of the electronic states of the underdoped regime. The optimal superconducting transition temperature for a specific material system will depend on another material specific energy-scale, such as the inter-plane block spin coupling suggested in ref. [36], along the c-axis.

Acknowledgments

References

[1] Batlogg B and Emery V J 1996 *Nature* **382** 20
[2] Li Z G, Feng H H, Yang Z Y, Hamed A, Ting S T, Hor P H, Bhavaraju S, DiCarlo J F and Jacobson A J 1996 *Phys. Rev. Lett.* **77** 5413
[3] Tokura Y, Torrance J B, Huang T C and Nazzal A I 1988 *Phys. Rev. B* **38** R7156
[4] Presland M R, Tallon J L, Buckley R G, Liu R S and Flower N E 1991 *Physica C* **176** 95
[5] Honma T, Hor P H, Hsieh H H and Tanimoto M 2004 *Phys. Rev. B* **70** 214517
[6] Obertelli S D, Cooper J R and Tallon J L 1992 *Phys. Rev. B* **46** R14928
[7] Radaelli P G, Hinks D G, Mitchell A W, Hunter B A, Wagner J L, Dabrowski B, Vandervoort K G, Viswanathan and Jorgensen J D 1994 *Phys. Rev. B* **49** 4163

[8] Ando Y, Hanaki Y, Ono S, Murayama T, Segawa K, Miyamoto N and Komiya S 2000 *Phys. Rev. B* **61** R14956

[9] Yamamoto A, Hu W. Z and Tajima S 2000 *Phys. Rev. B* **63** 024504

[10] Komiya S, Chen H D, Zhang S C and Ando Y 2005 *Phys. Rev. Lett.* **94** 207004

[11] Ando Y and Murayama T 1999 *Phys. Rev. B* **60** R6991

[12] Ando Y, Murayama T and Ono S 2000 *Physica C* **341-348** 1913

[13] Ando Y, Lavrov A N, Komiya S, Segawa K and Sun X F 2001 *Phys. Rev. Lett.* **87** 017001 ; Ando Y, Kurita Y, Komiya S, Ono S and Segawa K, 2004 *Phys. Rev. Lett.* **92** 197001

[14] Tamasaku K, Ito T, Takagi H and Uchida S 1994 *Phys. Rev. Lett.* **72** 3088

[15] Nishikawa T, Takeda J and Sato M 1995 *J. Phys. Soc. Jpn.* **63** 1441

[16] Hwang H Y, Batlogg B, Takagi H, Kao H L, Kwo J, Cava R J, Krajewski J J, Peck W F Jr. 1994 *Phys. Rev. Lett.* **72** 2636

[17] Tannar M A, Yefanov V S, Dyakin V V, Akimov A I and Chernyakova A 1991 *Physica C* **185-189** 1247

[18] Uchida S, Tamasaku K and Tajima S 1996 *Phys. Rev. B* **53** 14558

[19] Homes C C *et al*. 2004 *Nature* **430** 539

[20] Wang Y T and Hermann A M 2000 *Physica C* **335** 134

[21] Panagopoulos C, Xiang T, Anukool W, Cooper J R, Wang Y S, Chu C W 2003 *Phys. Rev. B* **67** R220502(R)

[22] Hofer J, Karpinski J, Willemin M, Meijer G I, Kopnin E M, Molinski R, Schwer L, Rossel C and Keller H 1998 *Physica C* **297** 103

[23] Kubo Y, Shimakawa Y, Manako T and Igarashi H 1991 *Phys. Rev. B* **43** 7875

[24] Izumi F, Jorgensen J D, Shimakawa Y, Kubo Y, Manako T, Pei Shiyou, Matsumoto T, Hitterman R L, Kanke Y 1992 *Physica C* **193** 426

[25] Tsvetkov A A, Schützmann J, Gorina J I, Kaljushnaia G A and Marel D van der 1997 *Phys. Rev. B* **55** 14152 ; Groen W A, de Leeuw D M and Stollman G M 1989 *Solid State Commun.* **72** 697

[26] Wagner J L, Radaelli P G, Hinks D G, Jorgensen J D, Mitchell J F, Dabrowski B, Knapp G S and Beno M A 1993 *Physica C* **210** 447

[27] Manako T Kubo Y and Shimakawa Y 1992 *Phys. Rev. B* **46** 11019

[28] Markiewicz R S and Kusko C 2002 *Phys. Rev. B* **65** 064520

[29] For example; Tallon J L and Loram J W 2001 *Physica C* **349** 53

[30] Sadewasser S, Schilling J S and Herman A M 2000 *Phys. Rev. B* **62** 9155

[31] Lorenz B, Li Z G, Honma T and Hor P H 2002 *Phys. Rev. B* **65** 144522

[32] Takeuchi T, Kondo T, Kitao T, Kaga H, Yang H, Ding H, Kaminski A and Campuzano J C 2005 *Phys. Rev. Lett.* **95** 227004

[33] Kittel C 2005 *Introduction to Solid State Physics, 8th Ed.* (New York: John Wiley & Sons) p 140

[34] Yoshida T *et al*. 2003 *Phys. Rev. Lett.* **91** 027001 ; Ino A *et al*. 2000 *Phys. Rev. B* **62** 4137

[35] Hor P H and Kim Y H 2002 *J. Phys.: Condens. Matter* **14** 10377

[36] Kim Y H and Hor P H 2006 *Mod. Phys. Lett. B* **20** 571